The ISME Journal (2007) 1, 678–692

www.nature.com/ismej

ORIGINAL ARTICLE

Streptococcus pyogenes serotype-dependent and independent changes in infected HEp-2 epithelial cells

Michael Klenk[1,3], Masanobu Nakata[1], Andreas Podbielski[1], Bianka Skupin[1], Horst Schroten[2] and Bernd Kreikemeyer[1]

[1]*Department of Medical Microbiology and Hospital Hygiene, Institute of Medical Microbiology, Virology and Hygiene, University Hospital Rostock, Schillingallee 70, Rostock, Germany and* [2]*Pediatric Infectious Diseases, Department of General Pediatrics, Heinrich-Heine-University, Düsseldorf, Germany*

The adherence, internalization and persistence of the human pathogen *Streptococcus pyogenes* (group A streptococci, GAS) to and within host cells were studied, and the induced responses of the infected epithelial cells were investigated. Next to common cellular responses on GAS infection, many responses of the infected HEp-2 epithelial cells are GAS serotype-specific. Moreover, several cellular responses do not correlate with the actual bacterial numbers adherent, internalized and persistent within the cells or the production of major cytolysins, as demonstrated for cytoskeletal pathways, cytokine release and apoptosis induction in infected cells. Measurement of activated caspases and caspase inhibition experiments uncovered activation of multiple caspase pathways by all GAS serotypes tested (M1, M3, M6 and M18). However, caspase 9 played a central role for M6 infections. During the persistence phase of the interaction, a differential and dynamic behavior of the infecting GAS serotype strains was found. After 14 h of host cell contact, all serotype strains caused host cell damage by virtually equal portions of apoptosis induction and necrosis mechanisms, as revealed by measurements of CK18Asp396/CK18 ratios. Between 14 and 24 h, persisting serotype M1 bacteria pertained this effect, whereas the serotype M6 GAS strain induced a major shift to necrotic mechanisms, and the serotype M3 and M18 GAS strains stimulated less necrosis, but shifted their host cells to apoptosis induction. Together, our study revealed that many cellular responses do not belong to general and uniform pathways, which are exploited by all GAS serotypes, explaining many of the already published discordant results.

The ISME Journal (2007) **1,** 678–692; doi:10.1038/ismej.2007.54; published online 18 October 2007
Subject Category: microbe–microbe and microbe–host interactions
Keywords: adherence; internalization; *S. pyogenes*; serotypes M1, M3, M6, M18; apoptosis; necrosis

Introduction

Streptococcus pyogenes (group A streptococci, GAS) is a very important and exclusively human pathogen. The annual global burden of GAS disease, including 111 million cases of pyoderma, over 616 million cases of pharyngitis and at least 517 000 deaths due to severe invasive diseases places this pathogen among the most important Gram-positive species with major impact in global mortality and morbidity (Bisno *et al.*, 2005; Carapetis *et al.*, 2005).

GAS classification and genotyping is based on *emm* typing, the gene encoding the M protein. More than 170 *emm*-types can currently be distinguished (Johnson *et al.*, 2006). Five major *emm* chromosomal patterns were identified based on the number and arrangement of *emm* subfamily genes (Facklam *et al.*, 1999). Of these, pattern A–D GAS strains are considered 'specialist', they are all serum-opacity factor (SOF)-negative, and are preferentially isolated from throat (pattern A–C: e.g. M1, M3, M6 and M18) or skin sites (pattern D). Pattern E strains (e.g. M49) are readily recovered from both tissues ('generalists') and are SOF-positive (Bessen *et al.*, 1996).

It remains unclear whether there are differences in colonization and infection capacities of these clustered serotype strains at their preferred tissue site. Although considered as classical extracellular pathogen, an increasing body of evidence established that GAS can adhere to and eventually internalize into eukaryotic cells. These traits are

Correspondence: B Kreikemeyer, Institute of Medical Microbiology, Virology and Hygiene, University Hospital Rostock, Schillingallee 70, Rostock 18055, Germany.
E-mail: Bernd.Kreikemeyer@med.uni-rostock.de
[3]Current address: Pediatric Infectious Diseases, Department of General Pediatrics, Heinrich-Heine-University, Düsseldorf, Germany.
Received 7 February 2007; revised 1 June 2007; accepted 4 June 2007; published online 18 October 2007

the first and subsequent steps in the infectious process, respectively, and are apparently independent of the tissue site preference of a given strain. The mechanisms of GAS cell adherence and invasion have been extensively studied and reviewed (Courtney *et al.*, 2002; Kreikemeyer *et al.*, 2004; Cleary, 2006). Several studies have investigated the cellular pathways required for the adherence and uptake process phenotypically (Pancholi and Fischetti, 1997; Miettinen *et al.*, 2000; Ozeri *et al.*, 2001; Purushothaman *et al.*, 2003; Wang *et al.*, 2006) and on the global transcriptome scale (Kobayashi *et al.*, 2003; Nakagawa *et al.*, 2004; Klenk *et al.*, 2005). Particularly, the early steps downstream of host cell adherence and internalization determine the fate of the invaded GAS and the infected cell, and are potentially crucial for the disease outcome. The decision, if the bacteria produce a locally contained infection, persist there for extended periods or spread from their initial infection site to cause severe systemic infections, is dependent on the environmental conditions, input signals, the mounted bacterial transcriptional response, and resulting phenotypical changes. In addition, this decision is influenced by the immediate response of the infected cell and the function and fitness of the host innate and adaptive immune systems. Adopting a systems biology point of view, several aforementioned events and aspects have been studied into detail (Musser and DeLeo, 2005).

The GAS dynamic transcriptome has been elucidated over the growth cycle *in vitro* in axenic culture medium (Beyer-Sehlmeyer *et al.*, 2005). Other studies have investigated the GAS transcriptome under *in vitro* conditions that mimic typical habitats GAS encounter *in vivo*. For example, GAS responds in a complex manner to growth in human saliva. Responsible proteins and regulators for pathogen survival (Sic, SpeB, SptR/S) have been studied through iterative expression microarray experiments (Shelburne *et al.*, 2005). Also, the GAS transcriptome essential for pathogen survival in human blood (Graham *et al.*, 2005) and the *ex vivo* dynamic transcriptional changes during experimentally induced pharyngitis in cynomolgus macaques have recently been examined (Virtaneva *et al.*, 2005).

On the eukaryotic side, the global transcriptional response in polymorphonuclear leukocytes (PMNs) that are important for later stages of the infection process, after uptake of GAS revealed an apparent acceleration of PMN apoptosis, leading to release of GAS and subsequent survival of the pathogens (Kobayashi *et al.*, 2003). A recent study from our group has investigated the dynamic transcriptional response of GAS-infected HEp-2 cells, using a serotype M49 GAS strain and an isogenic regulator mutant (Klenk *et al.*, 2005). Eighty-six HEp-2 cell genes were found differentially transcribed in wild type-infected cells, among them many genes encoding cytoskeletal proteins, cytokines, transcription factors and apoptosis-related factors (Klenk *et al.*, 2005).

In particular, apoptosis of GAS-infected epithelial cells is currently discussed in the context of tissue destruction, bacterial survival and spreading, and consequently as a prerequisite for systemic infection (Tsai *et al.*, 1999; Nakagawa *et al.*, 2001; Sierig *et al.*, 2003; Klenk *et al.*, 2005). Tsai *et al.* (1999) reported caspase 1 and caspase 3 induction during apoptosis in a process that depended on GAS internalization. GAS serotype M6 initiated apoptosis in HEp-2 cells via cytochrom-*c* release from mitochondria and caspase 9 activation in an internalization-dependent phenotype (Nakagawa *et al.*, 2001). An apoptosis induction in primary keratinocytes from an extracellular location, which involves dysregulation of intracellular calcium balance and ER stress, has recently been described for serotype M3 GAS strains and was found to depend on capsule and streptolysin O (SLO) expression (Cywes-Bentley *et al.*, 2005). In contrast to these observations, we reported HEp-2 cell apoptosis induction by a serotype M49 strain via caspase 2 activation pathways (Klenk *et al.*, 2005). Taken together, so far no uniform picture for apoptosis pathways and corresponding GAS serotype strains have been found. It remains unclear if serotype-dependent differences in apoptosis induction pathways exist.

Additionally, the question remains if host cell apoptosis supports bacterial dissemination. According to current concepts, all intracellular bacteria that initiate host cell apoptosis never reach the extracellular milieu, but instead are phagocytozed by neighboring macrophages together with the apoptotic cell remnants at late host cell apoptotic stages (Fink and Cookson, 2005). Such cellular deaths do not result in any inflammation. In contrast, host cell destruction by bacterial cytotoxic activities appears to provide better means to reach deep anatomical sites to cause systemic infection. Those lytic/necrotic mechanisms are normally associated with extensive inflammation (Fink and Cookson, 2005).

GAS uses several pathways to exert cytotoxic damage to host cells. Activity of the soluble secreted cytolysins streptolysin S (SLS) and SLO can cause major damage to host cells (Carr *et al.*, 2001; Nizet, 2002). SLO has been reported as part of a cytolysin-mediated translocation system that resembles type III secretion machines from Gram-negative bacteria. Pores formed by SLO facilitate translocation of NAD-glycohydrolase as effector molecule into the host cell cytoplasm (Madden *et al.*, 2001; Meehl *et al.*, 2006; Michos *et al.*, 2006). This system is under tight transcriptional control of the GAS Nra and MsmR global regulators, located in the fibronectin- and collagen-binding T antigen (FCT) pathogenicity island (Nakata *et al.*, 2005). It remains unclear whether any cytolysin predominantly contributes to the escape from the intracellular status of GAS.

Stimulated by these open questions, we intended to use a uniform infection model to elucidate

whether various GAS serotype strains induced different apoptotic pathways in exposed cells. Additionally, we sought to define whether transcriptional changes in the infected cell depend on the number of adherent and internalized GAS as well as their production of tissue/cell disruptive peptides. Finally, we investigated for the first time the temporal changes and dynamics in the ratio between GAS-induced host cell apoptosis and necrosis, which could potentially explain strain specific differences in the GAS–host cell interaction and the serotype-associated disease outcomes.

Materials and methods

Bacterial strains and cell culture conditions
GAS serotypes M1, M3, M6 and M18 were obtained from D Johnson, MN, USA (Podbielski *et al.*, 1999). Bacteria were cultured in TH broth and on TH agar (Unipath) both supplemented with 0.5% yeast extract (THY). GAS strains were cultured at 37°C under a 5% CO_2/20% O_2 atmosphere. The human laryngeal epithelial cell line HEp-2 (ATCC, CCL23) was cultured in Dulbecco's modified Eagle's medium (DMEM) supplemented with 10% FCS (both obtained from Life Technologies, Karlsruhe, Germany) at 37°C in an atmosphere containing 5% CO_2.

Adherence- and invasion-assay
For adherence and internalization assays, the HEp-2 cells were resuspended at a concentration of approximately 3×10^5 cells ml^{-1} in DMEM and seeded into 24-well tissue culture plates (Nunc, Wiesbaden, Germany), which were subsequently incubated for 24 h. For quantification of adherent/internalized GAS after 0.5 and 2 h, a standard assay was used (Molinari *et al.*, 2001). In control experiments, no significant growth of the different GAS serotype strains in the cell culture medium could be detected (data not shown). To determine the number of internalized bacteria at later time points, antibiotics (Molinari *et al.*, 2001) were added to kill all extracellular bacteria. The presence of intracellular viable bacteria was quantified at the time points 6, 10, 14 and 24 h post-infection (p.i.). For all subsequent assays using non-infected cells as control or for direct comparison, the cells were mock treated (antibiotics added whenever done for infected cells).

Real-time PCR
RNA quantification by real-time PCR was performed as published before (Klenk *et al.*, 2005). For the genes of interest, the full-length coding sequences were used for primer design (Primer Express 2.0, Applied Biosystems, Darmstadt, Germany). The nucleotide sequences of the chosen primer pairs (Thermo Electron, Ulm, Germany) are available in Supplementary Table S1. Signals (CT-values) for the genes of interest from each RNA sample were normalized to the signal for GAPDH in the same sample. The fold change of the sample from the infected HEp-2 cells was calculated relatively to the signal observed for non-infected HEp-2 cells. We prepared samples at 2, 6, 10, 14 and 24 h p.i. from GAS serotype M1-, M3-, M6- and M18-infected HEp-2 cells.

Cytokine measurements
The concentration of interferon (IFN)-γ and tomor necrosis factor (TNF)-α was determined in each supernatant from three independent infection experiments using the Bio-Plex Human Cytokine Analysis system with Panel A (de Jager *et al.*, 2003), according to the instructions of the manufacturer (Bio-Rad, Muenchen, Germany). The concentration of the cytokines was calculated from standard curves prepared for each cytokine, and values were normalized to the number of HEp-2 cells counted in each sample before the measurement (pg $\times 10^6$ cells). Specificity of the results was verified by proving non-existing crossreactivity of the antibodies included in the kit.

Measurement of activated caspases and determination of cytotoxicity
The determination of the time-dependent activation of caspases-2, -3, -8 and -9 in infected and non-infected HEp-2 cells were carried out as described before (Klenk *et al.*, 2005). The cytotoxicity of the M1, M3, M6 and M18 serotypes during infection compared with non-infected HEp-2 cells was measured by lactase dehydrogenase (LDH)-release from damaged cells, according to the instructions of the manufacturer (Roche, Mannheim, Germany).

Ratio of apoptosis to necrosis
To distinguish between apoptosis and necrosis in each sample at the same infection time point, the M30 ELISA and the M65 ELISA assays (PEVIVA AB, Bromma, Sweden) were used. During apoptosis, cytokeratin (CK) 18 is cleaved by caspases at the sites Asp238 and Asp396 and soluble CK18Asp396 is recognized by the M30-antibody ELISA (Leers *et al.*, 1999; Hagg *et al.*, 2002). Staurosporine (1 μM, Sigma, Steinheim, Germany)-treated HEp-2 cells were employed as positive controls for apoptosis induction (Binnicker *et al.*, 2003). The M65 ELISA measures total soluble CK18 protein, that is, the caspase-cleaved CK18Asp398 and uncleaved CK18. As a positive control for necrosis, HEp-2 cells were incubated with hydrogen peroxide (5 mM, Merck, Darmstadt, Germany) (McKeague *et al.*, 2003). The M30:M65 ratio determines the primary mode of cell death of the infected cells. Induction of apoptosis results in a high release of CK18Asp396, which is detected by M30 ELISA and M65 ELISA, a low CK18 release (detected only by M65) and results in a high

M30:M65 ratio. In opposite, increase of necrosis led to diminished release of CK18Asp396 and a strengthened secretion of CK18, resulting in a low M30:M65 ratio (Kramer *et al.*, 2004).

To study involvement of specific caspases during apoptosis, inhibition of the apoptotic program with different caspase inhibitors was studied. The HEp-2 cells were pre-incubated with (I) the general caspase inhibitor Z-VAD-FMK (20 μM solved in dimethylsufoxide (DMSO)), (II) the specific caspase 2 inhibitor Z-VDVAD-FMK (20 μM solved in DMSO) and (III) the specific caspase 9 inhibitor Z-LEHD-FMK (20 μM solved in DMSO) for 1 h.

Table 1a *Streptococcus pyogenes* serotypes M1, M3, M6 and M18 adherence to HEp-2 cells

Time	*Strain*	*% Of inoculum*	*Statistical significance*
Adherence and internalization (n = *3–6)*			
0.5 h	M1	2.8 ± 0.5	
	M3	3.5 ± 0.8	
	M6	3.2 ± 0.6	
	M18	4.1 ± 0.6	
Ranking:	M18 > M3 > M6 > M1		
2 h	M1	14 ± 4.8	*
	M3	46 ± 8.7	*
	M6	8.1 ± 1.9	
	M18	14 ± 3.0	*
Ranking:	M3 > M18 = M1 > M6		

Results are the mean ± s.d. of three to six separate experiments. *Significant difference to cells exposed to the other serotypes. The significance refers to *P*-values of <0.05.

Statistical analysis

The adherence and invasion assay (Tables 1a and b) were repeated on 3–6 completely independent occasions.

All real-time PCRs were repeated three times with RNA gained from three individual infection experiments (Table 2). The detection of secreted cytokines (Figure 1), the quantification of activated caspases (Figure 2), the determination of cytotoxicity by LDH release (Figure 3a) and the ratio of apoptosis (M30) to necrosis (M65) (Figure 3b) were each repeated three times from individual infection experiments.

For analysis of significant differences in these assays a Student's *t*-test was used. For each test, three significance levels were calculated (0.05, 0.01, 0.001). Due to the high complexity of the figures only *P*-values of <0.05 are shown.

Results

Comparison of adherence and internalization abilities

We previously evaluated the HEp-2 cell adherence and internalization capacity of a serotype M49 GAS pattern E strain (Bessen *et al.*, 1996; Klenk *et al.*, 2005). For the current comparative study, we first investigated the adherence, internalization efficiency and persistence of four pattern A–C GAS serotype strains, M1, M3, M6 and M18 (Tables 1a

Table 1b *Streptococcus pyogenes* serotypes M1, M3, M6 and M18 internalization into HEp-2 cells

Time	*Strain*	*% Of inoculum*	*Statistical significance*	*% Adhered cells (2 h) internalized*
Only internalization (n = *3–6)*				
6 h	M1	0.12 ± 0.07		0.9
	M3	15 ± 2.5	*	33
	M6	2.9 ± 1.0	*	36
	M18	0.6 ± 0.06	*	4.3
Ranking:	M3 > M6 > M18 > M1			
10 h	M1	0.008 ± 0.005		0.06
	M3	5.9 ± 1.8	*	13
	M6	1.2 ± 0.4	*	15
	M18	3.4 ± 0.2	*	24.3
Ranking:	M3 > M18 > M6 > M1			
14 h	M1	0.02 ± 0.01		0.14
	M3	1.7 ± 1.3	*	3.7
	M6	0.6 ± 0.4	*	7.4
	M18	0.1 ± 0.1		0.7
Ranking:	M3 = M6 > M18 > M1			
24 h	M1	0.08 ± 0.06		0.6
	M3	0.5 ± 0.3	*	1.1
	M6	0.2 ± 0.07	*	2.4
	M18	0.03 ± 0.01		0.2
Ranking:	M3 = M6 > M1 > M18			

Results are the mean ± s.d. of three to six separate experiments. *Significant difference to cells exposed to the other serotypes. The significance refers to *P*-values of <0.05.

Table 2 Changes of gene transcription in HEp-2 cells exposed to GAS assessed by quantitative real-time PCR

Gene designation	*Strain*	*2 h p.i.*	*6 h p.i.*	*10 h p.i.*	*14 h p.i.*	*24 h p.i.*
Transcription factors						
c-JUN	M1	7.7±2.2	—	—	5.1±2.2	2.6±0.7
	M3	15.7±7.3	7.3±23.1	2.3±0.1	4.5±1.7	6.4±0.9
	M6	—	2.5±0.4	2.5±0.5	5.3±2.7	4.1±1.0
	M18	3.0±0.2	—	—	—	3.8±0.8
FOSB	M1	—	—	—	4.9±0.7	—
	M3	5.8±0.8	8.0±2.7	—	—	—
	M6	—	—	—	−4.8±0.1	4.1±1.0
	M18	3.0±0.2	—	—	—	−3.5±0.1
ATF3	M1	4.9±2.6	—	—	7.6±6.8	—
	M3	8.8±2.6	7.2±1.7	3.8±2.6	18.9±1.3	—
	M6	—	—	3.8±2.8	—	−3.2±0.1
	M18	—	—	—	15.4±1.5	−3.6±0.1
NF-κB2	M1	7.6±0.6	7.2±0.8	9.3±2.4	—	—
	M3	8.7±2.7	3.0±0.1	—	—	—
	M6	2.5±0.5	—	—	—	—
	M18	5.6±1.2	—	—	—	—
NF-κBIA	M1	—	—	—	—	—
	M3	2.4±0.5	2.4±0.1	—	—	—
	M6	—	2.2±0.3	—	2.1±0.2	—
	M18	—	—	—	—	—
NOR-1	M1	—	—	—	—	—
	M3	2.6±0.1	3.7±1.5	—	—	—
	M6	—	2.6±0.8	—	—	—
	M18	—	—	—	—	—
Inflammation						
IL-6	M1	—	—	25.8±5.9	20.8±2.0	10.9±4.8
	M3	6.6±1.2	6.0±3.5	19.9±6.0	28.0±4.0	44.3±24.2
	M6	—	—	11.0±9.1	6.9±1.4	6.1±4.5
	M18	—	—	4.0±1.0	8.0±4.8	—
IL-8	M1	—	—	—	—	—
	M3	16.0±9.3	32.1±4.8	17.3±9.6	27.2±20.4	
	M6	—	—	8.8±2.2	—	8.6±0.2
	M18	—	—	—	9.3±1.0	—
Cytoskeleton						
GEM	M1	—	—	—	−7.0±0.1	—
	M3	3.8±1.1	3.9±1.6	19.3±5.2	—	—
	M6	—	—	—	—	−3.2±0.3
	M18	—	—	−6.4±0.1	—	—
ITGα 5	M1	—	—	3.1±0.1	—	—
	M3	—	—	3.5±0.7	—	3.5±1.8
	M6	—	—	—	—	—
	M18	—	—	—	—	—
Apoptosis						
PMAIP1	M1	—	—	—	−2.5±0.1	−2.8±0.1
	M3	—	3.4±0.1	4.4±0.1	4.9±3.1	3.5±2.2
	M6	—	4.0±1.9	7.9±1.0	3.2±0.0	—
	M18	—	—	3.6±1.6	—	—
GADD34	M1	2.5±0.4	2.4±1.1	2.6±1.0	—	—
	M3	4.4±2.2	7.9±1.9	6.9±3.6	3.1±0.4	—
	M6	2.3±0.6	5.1±3.2	3.7±1.5	—	—
	M18	3.0±0.7	2.5±0.7	—	—	—
OASL	M1	—	—	−3.2±0.1	—	—
	M3	—	—	6.4±5.4	35.0±2.8	8.7±5.4
	M6	—	2.0±0.2	17.8±3.6	23.0±3.9	5.8±0.5
	M18	—	2.0±1.2	5.4±0.7	16.0±4.5	3.6±0.5
TNFαiP3	M1	—	—	4.6±0.1	—	9.8±5.2
	M3	—	4.0±0.6	9.4±3.7	6.8±0.5	27.4±3.8
	M6	—	2.7±1.5	5.7±3.1	2.7±1.3	2.5±0.3
	M18	—	3.0±1.0	2.7±0.7	4.0±2.2	—

Abbreviations: ATF, activating transcription factor; FOSB, FBJ murine osteosarcoma viral oncogene homolog B; GADD, growth arrest and DNA damage-inducible protein; GAS, group A streptococci; GEM, GTP-binding mitogen-induced T-cell protein; IL, interleukin; ITG, integrin; NF, nuclear factor; NOR, neuron-derived orphan receptor; OASL, 2′-5′oligoadenylate synthetase like; PMAIP, phorbol-12-myristate-13-acetate-induced protein; RT-PCR, reverse-transcriptase PCR; —, no change.
The dynamic transcriptional changes of selected genes in HEp-2 cells exposed to the four GAS serotype strains investigated by real-time RT-PCR. To study the differential transcription of selected genes in infected HEp-2 cells, real-time RT-PCR was performed at time points 2, 6, 10, 14 and 24 h p.i.

and b; Supplementary Table S2). To allow valid interpretation of subsequent data, the different bacterial strains were synchronized by culture methods before exposure to the eukaryotic cells, and only results from those experiments were used in which the exact multiplicity of infection for all tested strains was experimentally confirmed. Using microscopic techniques, confounding effects by differences in bacterial chain length and the average number of infected HEp-2 cells between the strains were excluded (data not shown).

After infection of host cells, the number of adherent bacteria increases time dependently for all strains under investigation, reaching a maximum at 2 h p.i. Note that, at this time point, the serotype M3 GAS strain revealed the highest and the serotype M6 GAS strain the lowest adherence efficiency compared to the other serotypes. Serotypes M1 and M18 were nearly indistinguishable in their adherence capacity (Table 1a; Supplementary Table S2).

As a direct consequence, the number of internalized and persistent serotype M3 strain bacteria at

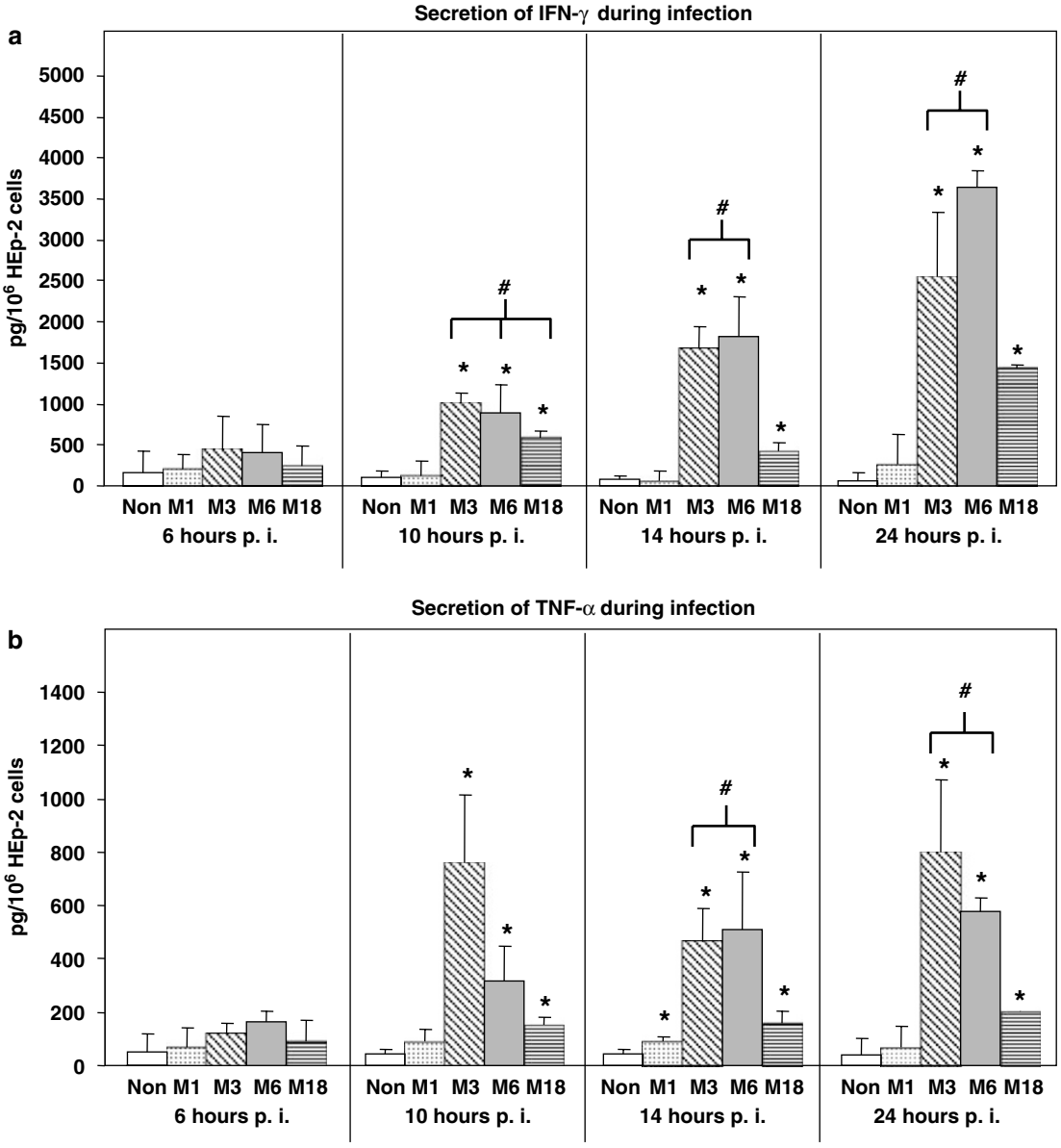

Figure 1 Measurement of cytokine release from GAS-exposed HEp-2 cells. HEp-2 cells infected with the GAS serotypes M1, M3, M6 and M18 secreted the cytokines IFN-γ (**a**), TNF-α (**b**), IL-6 (**c**) and IL-8 (**d**) into the supernatant. The concentration of each cytokine was related to the HEp-2 cell number and normalized to the basis of 10^6 cells. Results are the mean $\pm$ s.d. of three independent experiments. Symbols used are: *significant difference to non-infected cells and to cells exposed to the other serotypes; #no significant difference between the infected HEp-2 cells. 'Non', non-infected cells. Non-infected cells secrete significantly more IL-8 compared to cells infected with M1, M6 and M18 (**d**). The significance refers to *P*-values of <0.05. GAS, group A *streptococci*; IFN, interferon; IL, interleukin; TNF, tumor necrosis factor.

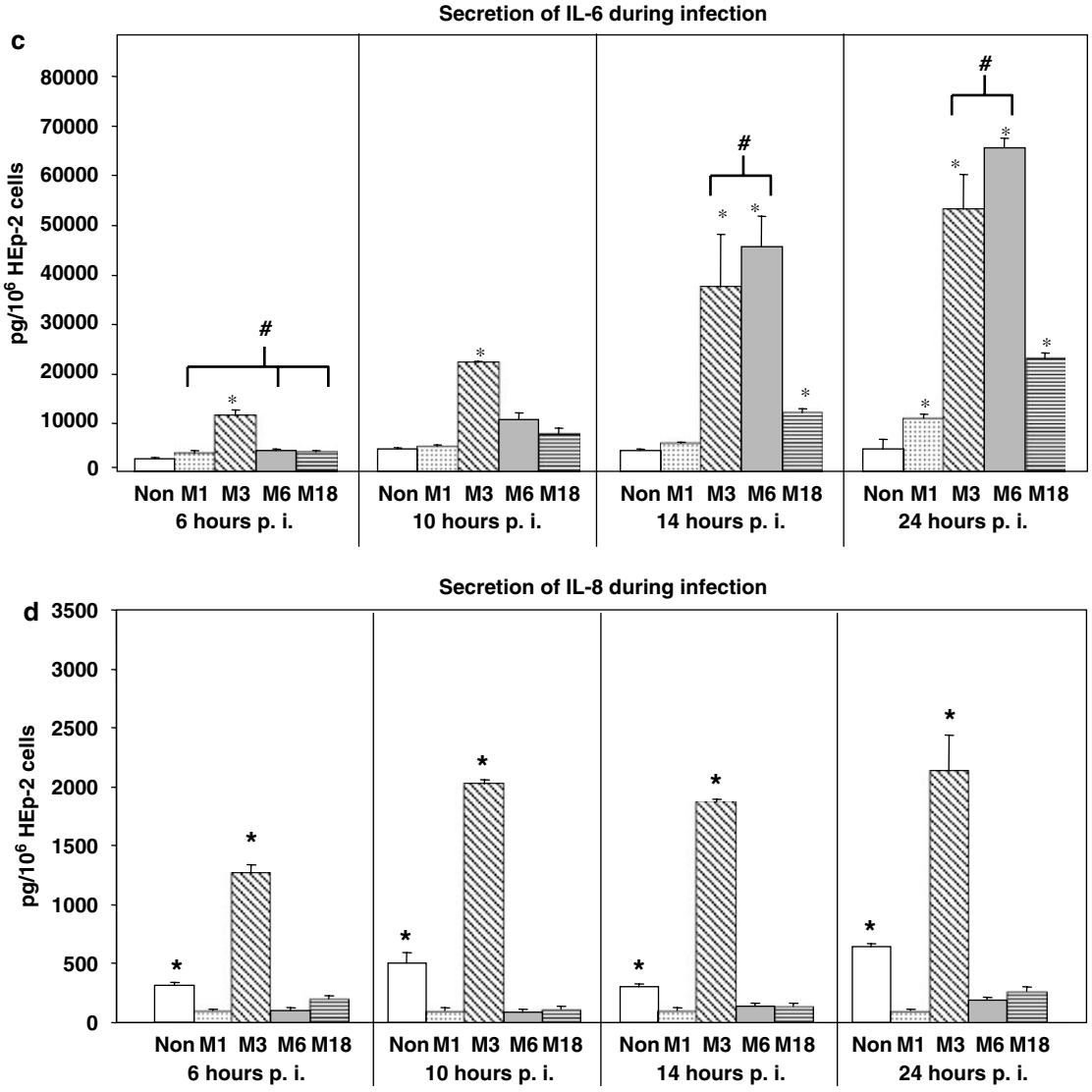

Figure 1 Continued.

6 h p.i. was the highest compared to the other bacteria (Table 1b; Supplementary Table S2). However, the percentage of the internalized and persistent M6 GAS bacteria is comparable to values obtained for the M3 GAS strain. In both infection experiments, approximately 30% of the initially adherent bacteria 2 h p.i. could be recovered from the internalized and persistent state after 6 h p.i. (Table 1b; Supplementary Table S2). Regardless of an initially higher adherence capacity of the GAS serotype M1 and M18 strains in comparison with M6-bacteria, the internalization and persistence of the two isolates was significantly lower compared to the serotype M6 strain. In direct comparison between M1 and M18 strains, the latter displayed a higher internalization and persistence rate.

The 10 h p.i. time point revealed the same significant differences as the 6 h p.i. time point. From 14 h p.i. on, both M3 and M6 GAS serotype strains were found to be more efficient in persistence in the infected cells as compared to M1 and M18 bacteria.

Differential transcriptional responses of infected cells in the categories transcription-factor-, cytokine-, cytoskeleton-, inflammation-, and apoptosis-related genes

Based on our previous results with HEp-2 cells that have been infected with a pattern E serotype M49 GAS strain, selected genes were studied by real-time PCR to investigate the temporal changes in the host cell response.

As shown in Table 2, we found an upregulation of c-JUN, of nuclear factor (NF)-κB2, as well as of the induced growth arrest and DNA damage-inducible protein 34, all of which are considered as part of the common apoptotic response. NF-κB2 transcription

appeared to be exclusively important for early stages of the bacteria–host cell interaction, since only serotype M1-infected host cells revealed a sustained induction up to 10 h p.i., thereby documenting serotype specificity and independence of the response from adherent and internalized bacterial numbers (Table 2). Particularly, serotype M6- and M18-infected HEp-2 cells responded by an upregulation limited to the early infection time points under investigation. Additionally, all serotypes induced transcriptional changes of the TNF-α corresponding responsive gene TNF-α-induced protein 3 (TNF-αiP3).

In contrast, the IFN-γ-inducible 2′-5′oligoadenylate synthetase like (OASL) and the phorbol-12-myristate-13-acetate-induced protein 1 mRNAs were found exclusively upregulated in host cells exposed to serotype M3, M6 and M18 GAS strains, but were downregulated in serotype M1 GAS-infected HEp-2 cells (Table 2). Furthermore, neuron-derived orphan receptor 1 and NF-κBIA (inhibitor A of NF-κB) were exclusively differentially transcribed in serotypes M3- and M6-infected HEp-2 cells (Table 2).

In good agreement with earlier observations in serotype M49-infected HEp-2 cells (Klenk *et al.*,

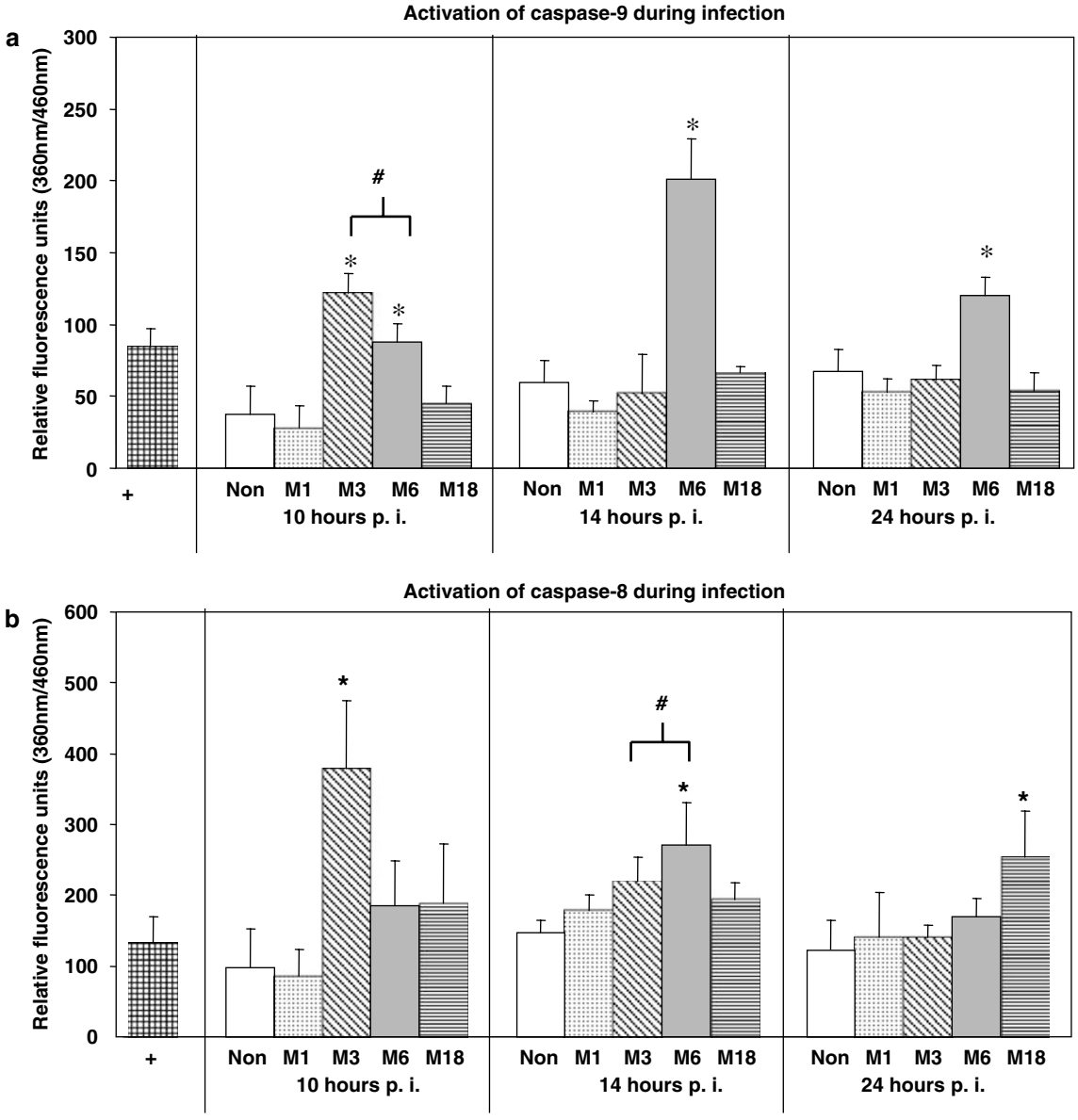

Figure 2 Quantification of activated caspases in HEp-2 cells exposed to GAS. The caspases 9 (**a**), 8 (**b**), 2 (**c**) and 3 (**d**) were activated during infection of HEp-2 cells with the GAS serotype strains M1, M3, M6 and M18. Results are the mean$\pm$s.d. of three separate experiments. Symbols used are: *significant difference to non-infected cells and to cells exposed to the other serotypes; #no significant difference between the infected HEp-2 cells; $^{+}$staurosporin treatment was used as positive control. The significance refers to *P*-values of <0.05. GAS, group A *streptococci*.

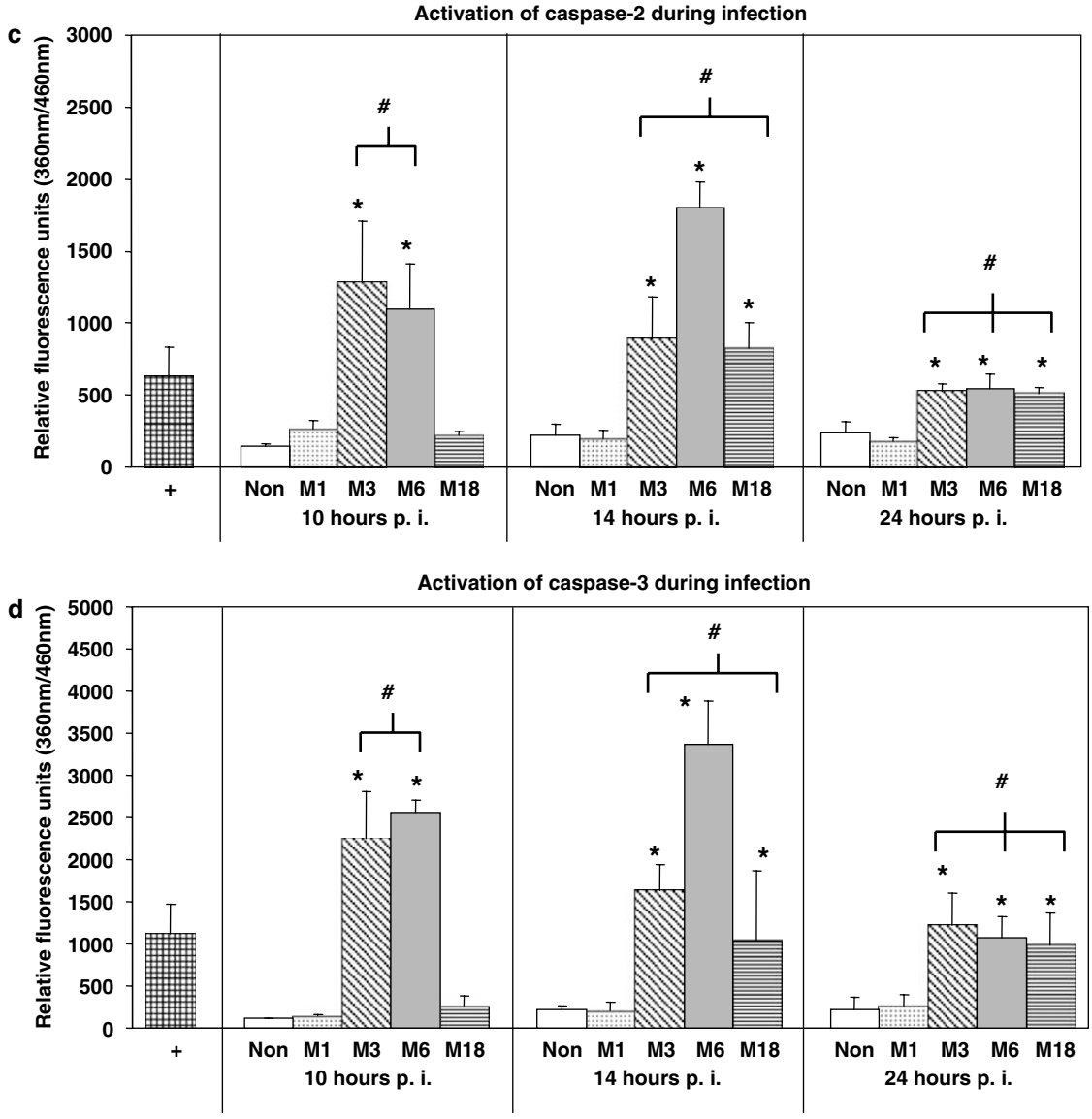

Figure 2 Continued.

2005), we found significant transcriptional induction of genes encoding IL-6 and -8 (Table 2), although the actual amounts of secreted pro-inflammatory cytokines from the infected cells differed markedly between the strains (see next section, Figure 1; Supplementary Table S2).

For genes encoding cytoskeletal proteins GEM (GTP-binding mitogen-induced T-cell protein) and ITGα-5 (integrin-α5), more diverse and serotype-dependent phenotypes emerged (Table 2). Only the serotype M3 strain was able to induce transcription of genes encoding GEM and ITGα-5, thereby leading to the same host cell phenotype as M49 bacteria in previous experiments (Klenk *et al*., 2005). Serotype M1 repressed GEM transcription and induced ITGα-5 transcription during the persistence phase of the host cell interaction, whereas M6 and M18 repressed GEM transcription and had no effect on transcription of the gene encoding ITGα-5 (Table 2).

Together, these results document that many cellular pathways are exploited by all serotypes tested here (M1, M3, M6, M18) and in our previous study (M49, Klenk *et al*., 2005). However, many of the actual transcriptional changes in the infected cells are serotype dependent and do not correlate well with the adherence and internalization capacities of the GAS serotypes tested.

The cytokine profile during the infection of HEp-2 cells

In good agreement with the reported transcriptional induction of OASL and TNF-αiP3, significant amounts of IFN-γ and TNF-α, respectively, were exclusively secreted by serotypes M3-, M6- and M18-infected cells. This suggested that in fact cytokine release and transcriptional induction of genes encoding responsive proteins are linked (Figures 1a and b).

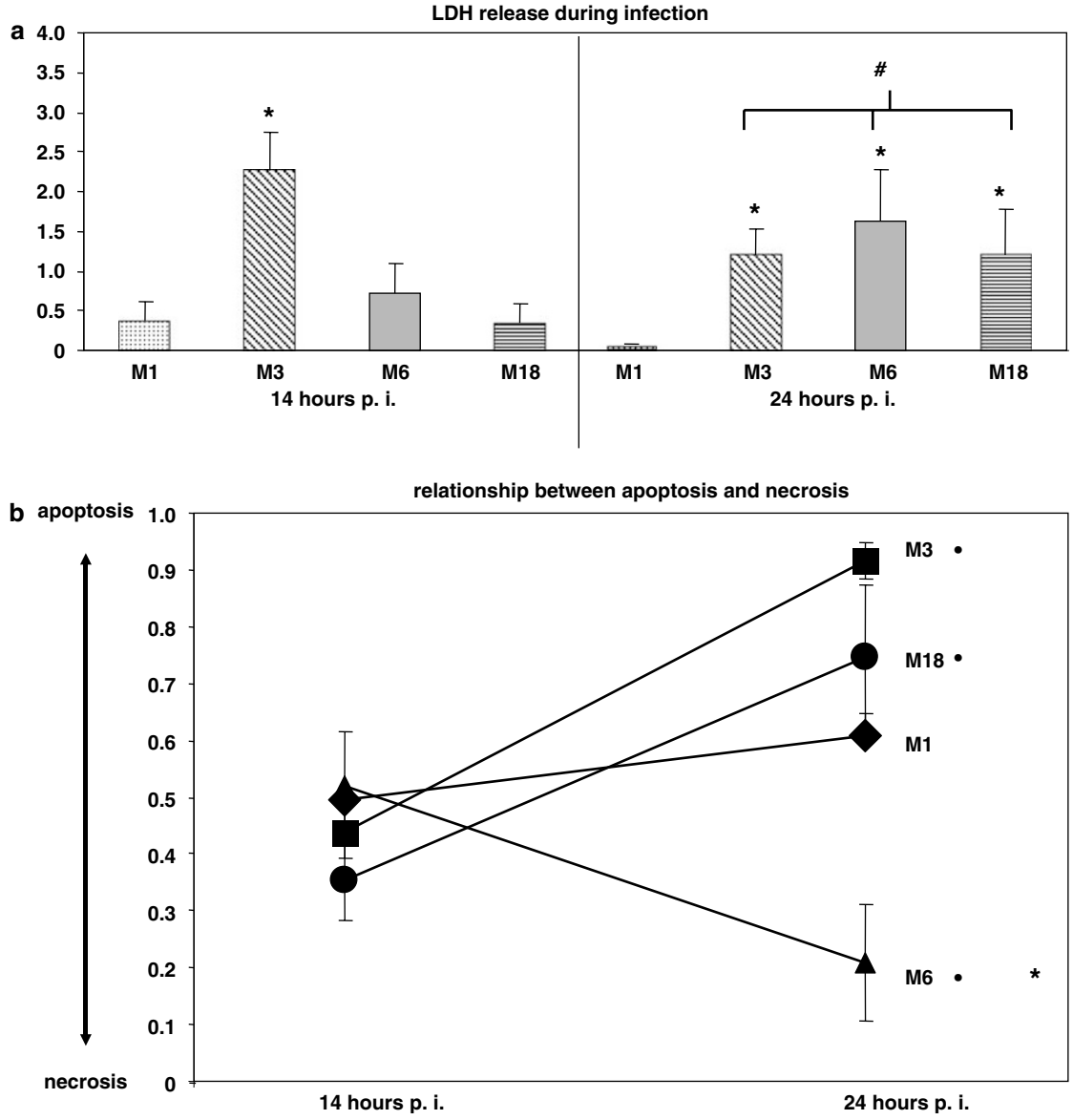

Figure 3 Measurement of LDH, CK18, and CK18Asp396 secretion into the supernatant of HEp-2 cells exposed to the four GAS serotype strains. Determination of LDH released by damaged HEp-2 cells into the supernatant (**a**). During necrosis, CK18 is mainly released by infected cells, whereas during apoptosis CK18 is cleaved to CK18Asp396, which in turn is found in higher concentration in the supernatant. The ratio of CK18Asp396 to CK18396 + CK18 is an indicator for apoptosis (high levels of CK18ASP396) and for necrosis (low levels of CK18Asp396) (**b**). Results are the mean ± s.d. of three independent experiments. Symbols used are: *significant difference to non-infected cells and to cells exposed to the other serotypes; •significant difference between 14 and 24 h. The significance refers to *P*-values of <0.05. CK, cytokeratin; LDH, lactase dehydrogenase.

In contrast, HEp-2 cells exposed to serotype M1 did not release significantly different IFN-γ amounts when compared to non-infected cells (Figure 1a). All infected cells secreted TNF-α at higher levels compared to non-infected cells (Figure 1b). Exposure of host cells to serotypes M3 and M6 strains induced higher IFN-γ and TNF-α secretion levels as compared to HEp-2 cells infected with M1 and M18 GAS serotype strains. No significant differences could be detected for M3- and M6-exposed cells for these two cytokines (Figures 1a and b).

Similar to the TNF-α secretion, all strains induced the release of IL-6 in a significant higher concentration compared to non-infected cells (Figure 1c). Not unexpectedly, from 14 h p.i. host cells when exposed to both M3 and M6 serotype showed a significant higher IL-6 release compared to the two other serotype strains. However, surprisingly, only HEp-2 cells exposed to serotype M3 released significant higher IL-8 amounts compared with non-infected cells (Figure 1d). In contrast, infection of host cells with serotypes M1, M6 and M18 lead to

secreted IL-8 levels, which were constantly and significantly lower compared to those secreted from non-infected cells.

Thus, apart from the IL-8 response, the strength of cytokine release by the infected cells is obviously dependent on the adherence and internalization capabilities of the individual GAS serotypes, and in consequence, is directly linked to bacterial numbers (Supplementary Table S2).

Caspase activation in GAS-infected HEp-2 cells

Preliminary results indicated that significant activation of caspases only occurred at later stages of the host cell infection (Klenk *et al.*, 2005). Thus, only 10, 14 and 24 h p.i. were investigated in more detail. Exposure of the HEp-2 cells to the four GAS strains under investigation and treatment of the cells with staurosporine (positive control) subsequently led to the activation of the caspases 9, 8, 2 and 3 in a time-dependent manner (Figures 2a–d). Of all investigated initiator caspases, in the presence of all four GAS strains, caspase 2 displayed the highest (five-fold) increase of its activation level, whereas activation of caspases 9 and 8 varied between the isolates. Infection of HEp-2 cells with GAS serotype M1 and M18 strains did not result in any significant activation of caspase 9, which apparently plays an exclusive role in serotype M6 infection pathways and the early stages of serotypes M3 host cell interaction (Figure 2a). Also note that the infection of HEp-2 cells with serotype M1 did not lead to any significant activation of all caspases investigated here, although these bacteria were shown to adhere, internalize and persist in HEp-2 cells in significant numbers (Tables 1a and b, Supplementary Table S2). The significant highest activation level of caspase 8 was found in cells exposed to serotype M3 GAS after 10 h p.i. On exposure of host cells to GAS serotype M3 and M6 strains, a significant amount of activated caspases 9, 2, and 3 could be detected, suggesting the recruitment of several apoptosis pathways in infected cells by these serotypes. Remarkably, cells infected with serotype M6-bacteria generated a significant higher activation of the caspases 9, 2 and 3 than cells exposed to serotype M3-bacteria, although the absolute numbers of adherent and internalized M6 bacteria are significantly lower at each infection time point investigated.

Again, these results documented in part a serotype-specificity of the host cell reaction, the exploitation of several apoptotic pathways by one single serotype, and the independence of the host cell apoptosis reaction from the initial number of infecting bacteria.

The temporal proportion and dynamics of necrosis and apoptosis in GAS-infected epithelial cells

Next, we determined the predominant mechanism by which host cells are damaged by adherent and internalized GAS strains. We measured the temporal changes in the proportion of apoptosis versus necrosis using material from the same infection experiment. As a first approach to determine cytotoxic effects, the cytotoxicity of M1, M3, M6 and M18 bacteria during infection compared to non-infected HEp-2 cells was determined by means of LDH release (Figure 3a).

The temporal LDH secretion from cells infected with serotype M1 was significantly lower compared to cells infected with the other serotypes. Cells exposed to the serotype M3 strain revealed massive cytotoxic damage at 14 h p.i., indicated by high amounts of released LDH. Remarkably, decreased LDH levels were found in HEp-2 cells infected with serotype M1 and M3 GAS strains from 14 to 24 h p.i. In contrast, the LDH release after infection with M6 and M18 bacteria increased from 14 to 24 h p.i.

To assess the ratio of apoptosis and necrosis induction, we used a method which determined the ratio of CK18Asp396 (caspase-cleaved CK18) to the sum of un-cleaved CK18 and CK18Asp396. With this method, a high ratio is a strong indicator that cell death is mainly caused by apoptosis induction, and a low ratio indicates predominant death of the cells via lytic/necrotic damage (Figure 3b).

A more or less equal contribution of apoptosis and necrosis to cell death was detected at 14 h p.i. in cells infected with all four GAS serotype strains. Apparent differences in the development of this ratio among the serotypes could be noticed between 14 h p.i. and 24 h p.i. At these infection time points, the host cells exposed to the serotypes M3 and M18 bacteria predominantly caused cell death by induction of the apoptotic program, whereas cells exposed to the serotype M6 GAS strain revealed a major shift to cell death mechanisms induced by lysis/necrosis. Finally, values of released CK18Asp396 and CK18 from cells infected with serotype M1 bacteria remained unchanged and did not reveal any significant shifts in either direction during the investigated infection period. It is noteworthy to say that, in this particular assay, the values for M1-infected cells were always close to the lower detection limit of the assay (determined by a standard curve), suggesting a hardly detectable activation of caspases. However, since the values were still in the linear range of the assay, we decided to include the data converted to ratio values.

As shown in Supplementary Figure S1, pretreatment of HEp-2 cells with a general caspase inhibitor basically blocked apoptosis mechanisms induced by all serotype strains at 24 h p.i. and shifted the response of the infected cells to necrosis. Inhibition of caspase-2 did not have any significant effects, supporting the earlier observation that all serotypes simultaneously induce several different apoptosis pathways. Only GAS serotype M6-infected cells showed a significant reduction of apoptosis activity in case caspase-9 was blocked, suggesting a more

predominant role for caspase-9 in serotype M6 infections.

Discussion

The adherence to and internalization into host epithelial cells is one of the major pathways by which GAS initiate host colonization after entering the body. These initial steps of the infection process are decisive on the progression and outcome of the infection. Almost all investigated GAS serotypes have been shown to interact with host epithelial cells by one of several ways. The host cells respond by changing and adapting transcription of many genes to combat the intruding bacteria, and in most cases either die by bacteria-inferred cytotoxic mechanisms or by initiation of the host cell death program.

Two major questions we wanted to address in this study were, if the host cell transcriptional response as well as the dynamics of cytotoxic and apoptosis pathways are serotype specific, and if these processes also depend on the number of adherent, invading and persistent bacteria.

As shown in this study, the capacities of the different serotype GAS strains to adhere to, internalize into, and finally to persist for up to 24 h in HEp-2 epithelial cells is diverse. During the adherence phase, serotypes M1 and M18 strains were indistinguishable. After internalization and during persistence, the M1 strain died at a high rate, whereas the M18 strain survived and even multiplied between 6 and 14 h p.i. The adherence, internalization and persistence behavior of the serotype M3 strain was comparable to published results for serotype M49 (Klenk *et al.*, 2005). A possible explanation for this phenotypical similarity is the presence of the same type of FCT-pathogenicity region in both strains' chromosome (Bessen and Kalia, 2002; Kreikemeyer *et al.*, 2004). Next, to several other factors (Courtney *et al.*, 2002; Courtney and Podbielski, 2006), the FCT-region has repeatedly been demonstrated to provide means for adherence and internalization mechanisms. Recent publications have shown that many genes from the FCT-pathogenicity region are required for the formation and expression of GAS pilus-like structures (Mora *et al.*, 2005) and that similar genomic regions and pilus-like structures are present in the closely related group B streptococci and pneumococci (Lauer *et al.*, 2005; Dramsi *et al.*, 2006; Rosini *et al.*, 2006; Telford *et al.*, 2006). At least many of the differences in adherence observed for serotypes M1, M6, M18 and M3 isolates could potentially be attributed to the gene content of the respective FCT-pathogenicity regions present in those serotypes and the types of pili that are expressed from the FCT-encoded genes. However, so far, thorough experimental evidence for pilus involvement in adherence and internalization mechanisms is still missing, and the general influence of pili on the infectious process remains difficult to understand (Telford *et al.*, 2006).

Although the serotype M6 isolate displayed the lowest initial adherence and internalization numbers after 2 and 6 h p.i., judged from its intracellular colony-forming units (CFU) counts after 24 h co-culture, this particular serotype appears to be well equipped for intracellular survival and persistence. Additionally, in spite of an initially low attachment rate this serotype strain managed to get almost 30% of the adherent bacterial population internalized into the cells after 6 h and thus, compared to rates of the M3 strain, which showed much higher initial attachment rates. The general trends in adherence/internalization/persistence capacities (M3 > M6 > M18 > M1, see Tables 1a and b; Supplementary Table S2) were also reflected in several of the cellular changes measured in the infected HEp-2 cells. A cellular response that is apparently dependent on the number of adherent, invading and persisting bacteria is the release of the cytokines IFN-γ, TNF-α and IL-6.

In contrast, the most impressive parameter of serotype-specific changes in host cell response is the secretion of IL-8. This pro-inflammatory cytokine is important for the recruitment of defense cells to the infection site. However, only serotype M3 stimulated significant release of IL-8 from infected cells, whereas all other serotypes induced IL-8 amounts even lower than those secreted from non-infected cells. The recent description and partial characterization of a IL-8 protease expressed by GAS could potentially explain this phenotype (Hidalgo-Grass *et al.*, 2004; Edwards *et al.*, 2005). Apparently, serotypes M1, M6 and M18 could produce high amounts of this specific protease, leading to efficient digestion of IL-8 secreted form the infected cells. Alternatively, these phenotypic differences are due to a serotype-specific transcriptional regulation of the IL-8 protease encoding gene in these serotypes (Klenk *et al.*, 2005). This phenotype would lead to a major advantage for pathogen survival at the site of infection.

One major finding of this study is the obvious independence of many of the transcriptional changes in the infected cells from the efficiency of adherence, internalization and persistence of the infecting GAS strains. This suggests that many observed changes are a genuine trait of the host cell and that many of those host cell responses are apparently rather dependent on specific virulence factors expressed by the various serotype strains investigated here, than uniform responses after adherence, internalization and persistence. This is particularly apparent in the transcriptional response of the infected cells if serotype M3 and M6 inferred differential host cell gene transcription is analyzed, as well when host cell transcription upon M1 and M18 infection is compared. Based on commercially available genome sequences of the GAS serotypes

studied here, the gene context and content of the 'core' or 'backbone' chromosome is very similar. In contrast, the gene content and position of prophages are variable among different serotypes and potentially explain the diversity (Banks *et al.*, 2004). Particularly the serotype-dependent variability of virulence factors encoded on prophages, including superantigens, DNAses, hyaluronidases, phospholipase A_2, is a possible explanation for the diversity in the host cell responses.

Another category of host cell factors responding in a serotype-specific manner comprise GEM and ITGα5, genes which encode for a small GTP-binding protein and the fibronectin-binding integrin, respectively. Both proteins are involved in cytoskeletal rearrangements. Again, the transcriptional induction following M3 exposure is indistinguishable from the recently published results for M49, which in addition to increased GEM- and ITGα5-transcription induced RhoA-pathways during the adherence and internalization process (Klenk *et al.*, 2005). This could be explained by the eukaryotic cell binding of both strains via the protein F2 major adhesin.

For cells exposed to serotype M6 isolates, RhoA was not involved in the adherence and uptake process (Ozeri *et al.*, 2001) and protein F1 was found to be the major adhesin for host cell internalization (Hanski and Caparon, 1992). Since GEM would activate GEM-interacting protein and subsequently RhoA, the now demonstrated lack of GEM transcriptional induction in serotype M6-infected cells confirmed the earlier observations by Ozeri *et al.* (2001). Serotype M1 strains do not encode a fibronectin-binding protein in their FCT-region, potentially explaining their apparent phenotype. Serotype M18 isolates generally share all the genes of the FCT-region with M3 and M49 (Bessen and Kalia, 2002; Kreikemeyer *et al.*, 2004), although the individual gene sequences differ up to 30%. Since the M18 strain induced a divergent phenotype in transcriptional induction and repression of factors involved in cytoskeletal re-arrangements, this pattern could be due to this sequence variability.

After host cell adherence and internalization, apoptosis in GAS-infected host cells has been reported (Tsai *et al.*, 1999; Nakagawa *et al.*, 2001, 2004; Cywes-Bentley *et al.*, 2005; Klenk *et al.*, 2005) and is discussed as an advantageous mechanism for the bacteria to avoid killing, and thereby supporting spread of the bacteria to internal anatomical sites. However, it is still unclear if this hypothesis is correct, since apoptosis is a sequential process in which the cytoplasmic content is not released, and thereby does not led to inflammation. Rather, apoptotic bodies and cell remnants are taken up and are subsequently degraded if *in vivo* professional phagocytes are present (Fink and Cookson, 2005). Bacterial cytotoxic activity exerted from outside or within the cells appears to be more potent in cell and tissue destruction, thereby opening barriers to bacterial spread and induction of inflammation. Consequently, the degree of apoptosis- and necrosis-based damage after GAS host cell adherence, internalization and persistence is apparently critical for disease outcomes and was measured.

Some discordant results were obtained for M1- and M6-infected HEp-2 cells in the two separate apoptosis assays (activation of caspases, ratio apoptosis/necrosis). These discrepancies are most likely due to the different assay profiles, sensitivities and specificities. However, we conclude that host cell apoptosis factors were found to form another category of serotype-dependent molecules, as already suspected from earlier discordant results (Nakagawa *et al.*, 2001; Klenk *et al.*, 2005). Results from an earlier study of Nakagawa and co-workers were confirmed in this study, since only serotype M6 bacteria significantly activated caspase 9 in infected HEp-2 cells throughout the complete investigation period. However, in extension to observations by Nakagawa and co-workers, the serotype M6 isolate apparently activated other apoptotic pathways, including caspases 2- and 8-dependent ones. The serotype M1 strain was unable to activate measurable amounts of all caspases investigated. In contrast, serotypes M3 and M18 strains activated caspases from at least two pathways (caspase 2 and 8), in consequence merging into activation of the central caspase 3. The induction of multiple pathways was not found in serotype M49 GAS-infected host cells (Klenk *et al.*, 2005) and therefore underscores the serotype specificity of some host cell responses, in addition to the independency of many host cell responses from actual numbers of adherent and internalized bacteria.

Another finding of this study stemmed from the investigation of temporal changes in host cell apoptosis and necrosis. Apparently, various GAS serotype strains prefer different routes to inflict host cell damage. Serotype M3 and M18 strains mainly induced host cell apoptosis, suggesting a potential efficient killing and elimination of these serotype strains during tissue infection. In contrast, serotype M6 mainly induced damage to host cells by lytic/necrotic mechanisms. This is potentially caused by either a dynamic increase in extracellular cytotoxcicity or effective release of internalized and persistent bacteria for a new infection round or spreading. Yet, the observed changes in host cell viability did not correlate with the presence of the major GAS cytolysins SLS and SLO in our cell culture supernatants (data not shown). It is conceivable that other factors released and secreted from GAS during host cell contact could also lead to necrotic damage.

In summary, we have shown that the response of the infected host cell is composed of parts that are exploited by all tested serotypes in uniform ways and in dependence on actual bacterial numbers infecting the cells. Another part of the responses of GAS-infected host cells are in contrast

serotype-dependent, but within the ranges of our experimental results apparently independent of actual bacterial numbers adhering, internalizing and persisting in infected cells. A correlation between the dynamic GAS serotype-dependent behavior in terms of host cell apoptosis and necrosis induction in these *in vitro* experiments with *in vivo* processes needs to be determined in future studies and will hopefully lead to a better understanding of GAS infections.

Acknowledgements

This work was supported by a grant from the DFG-(Deutsche Forschungsgemeinschaft) Priority Program 1047 (Ecology of Bacterial Pathogens: Molecular and Evolutionary Aspects) awarded to BK (KR 1765/2-1). This work was in part supported by a grant from the German BMBF in the framework of the ERANet Pathogenomics network awarded to BK. The authors would like to acknowledge the expert technical assistance of Jana Norman, Yvonne Humboldt and Anne Eckhardt. We acknowledge Burkhard Krüger for granting access to the cytofluor 2350 (Millipore, Schwalbach, Germany) and Christian Zimmermann from BioRad Laboratories for providing access to the Bio-Plex Suspension Array system.

References

Banks DJ, Porcella SF, Barbian KD, Beres SB, Philips LE, Voyich JM *et al.* (2004). Progress toward characterization of the group A *streptococcus* metagenome: complete genome sequence of a macrolide-resistent serotype M6 strain. *J Infect Dis* **190**: 727–738.

Bessen DE, Kalia A. (2002). Genomic localization of a T serotype locus to a recombinatorial zone encoding extracellular matrix-binding proteins in *Streptococcus pyogenes*. *Infect Immun* **70**: 1159–1167.

Bessen DE, Sotir CM, Readdy TL, Hollingshead SK. (1996). Genetic correlates of throat and skin isolates of group A streptococci. *J Infect Dis* **173**: 896–900.

Beyer-Sehlmeyer G, Kreikemeyer B, Horster A, Podbielski A. (2005). Analysis of the growth phase-associated transcriptome of *Streptococcus pyogenes*. *Int J Med Microbiol* **295**: 161–177.

Binnicker MJ, Williams RD, Apicella MA. (2003). Infection of human urethral epithelium with *Neisseria gonorrhoeae* elicits an upregulation of host anti-apoptotic factors and protects cells from staurosporine-induced apoptosis. *Cell Microbiol* **5**: 549–560.

Bisno AL, Rubin FA, Cleary PP, Dale JB. (2005). Prospects for a group A steptococcal vaccine: rationale, feasibility, and obstacles—report of a national institute of allergy and infectious diseases workshop. *Clin Infect Dis* **41**: 1150–1156.

Carapetis JR, Steer AC, Mulholland EK, Weber M. (2005). The global burden of group A streptococcal diseases. *Lancet Infect Dis* **5**: 685–694.

Carr A, Sledjeski DD, Podbielski A, Boyle MD, Kreikemeyer B. (2001). Similarities between complement-mediated streptolysin S-mediated hemolysis. *J Biol Chem* **276**: 41790–41796.

Cleary PP. (2006). *Streptococcus* moves inward. *Nat Med* **12**: 384–386.

Courtney HS, Hasty DL, Dale JB. (2002). Molecular mechanisms of adhesion, colonization, and invasion of group A *streptococci*. *Ann Med* **34**: 77–87.

Courtney HS, Podbielski A. (2006). Group A streptococcal invasion of host cells. In: Lamont RJ (ed). *Bacterial Invasion of Host Cells*. Cambridge University Press.

Cywes-Bentley C, Hakansson A, Christianson J, Wessels MR. (2005). Extracellular group A *Streptococcus* induces keratinocyte apoptosis by dysregulating calcium signalling. *Cell Microbiol* **7**: 945–955.

de Jager W, te Velthuis H, Prakken BJ, Kuis W, Rijkers GT. (2003). Simultaneous detection of 15 human cytokines in a single sample of stimulated peripheral blood mononuclear cells. *Clin Diagn Lab Immunol* **10**: 133–139.

Dramsi S, Caliot E, Bonne I, Guadagnini S, Prevost MC, Kojadinovic M *et al.* (2006). Assembly and role of pili in group B streptococci. *Mol Microbiol* **60**: 1401–1413.

Edwards RJ, Taylor GW, Ferguson M, Murray S, Rendell N, Wrigley A *et al.* (2005). Specific C-terminal cleavage and inactivation of interleukin-8 by invasive disease isolates of *Streptococcus pyogenes*. *J Infect Dis* **192**: 783–790.

Facklam R, Beall B, Efstratiou A, Fischetti V, Johnson D, Kaplan E *et al.* (1999). Emm typing and validation of provisional M types for group A *streptococci*. *Emerg Infect Dis* **5**: 247–253.

Fink SL, Cookson BT. (2005). Apoptosis, pyroptosis, and necrosis: Mechanistic description of dead and dying eukaryotic cells. *Infect Immun* **73**: 1907–1916.

Graham MR, Virtaneva K, Porcella SF, Barry WT, Gowen BB, Johnson CR *et al.* (2005). Group A *Streptococcus* transcriptome dynamics during growth in human blood reveals bacterial adaptive and survival strategies. *Am J Pathol* **166**: 455–465.

Hagg M, Biven K, Ueno T, Rydlander L, Bjorklund P, Wiman KG *et al.* (2002). A novel high-through-put assay for screening of pro-apoptotic drugs. *Invest New Drugs* **20**: 253–259.

Hanski E, Caparon MG. (1992). Protein F, a fibronectin-binding protein, is an adhesin of the group A streptococcus (*Streptococcus pyogenes*). *Proc Natl Acad Sci* **89**: 6172–6176.

Hidalgo-Grass C, Dan-Goor M, Maly A, Eran Y, Kwinn LA, Nizet V *et al.* (2004). Effect of a bacterial pheromone peptide on host chemokine degradation in group A streptococcal necrotising soft-tissue infections. *Lancet* **363**: 696–703.

Johnson DR, Kaplan EL, VanGheem A, Facklam RR, Beall B. (2006). Characterization of group A streptococci (*Streptococcus pyogenes*): correlation of M-protein and emm-gene type with T-protein agglutination pattern and serum opacity factor. *J Med Microbiol* **55**: 157–164.

Klenk M, Koczan D, Guthke R, Nakata M, Thiesen HJ, Podbielski A *et al.* (2005). Global epithelial cell transcriptional responses reveal *Streptococcus pyogenes* Fas regulator activity association with bacterial aggressiveness. *Cell Microbiol* **7**: 1237–1250.

Kobayashi SD, Braughton KR, Whitney AR, Voyich JM, Schwan TG, Musser JM *et al.* (2003). Bacterial pathogens modulate an apoptosis differentiation program in human neutrophils. *Proc Natl Acad Sci USA* **100**: 10948–10953.

Kramer G, Erdal H, Mertens HJ, Nap M, Mauermann J, Steiner G *et al.* (2004). Differentiation between cell death modes using measurements of different soluble forms of extracellular cytokeratin 18. *Cancer Res* **64**: 1751–1756.

Kreikemeyer B, Klenk M, Podbielski A. (2004). The intracellular status of *Streptococcus pyogenes*: role of extracellular matrix-binding proteins and their regulation. *Int J Med Microbiol* **294**: 177–188.

Lauer P, Rinaudo CD, Soriani M, Margarit I, Maione D, Rosini R *et al.* (2005). Genome analysis reveals pili in Group B *Streptococcus*. *Science* **309**: 105.

Leers MP, Kolgen W, Bjorklund V, Bergman T, Tribbick G, Persson B *et al.* (1999). Immunocytochemical detection and mapping of a cytokeratin 18 neo-epitope exposed during early apoptosis. *J Pathol* **187**: 567–572.

Madden JC, Ruiz N, Caparon M. (2001). Cytolysin-mediated translocation (CMT): a functional equivalent of type III secretion in gram-positive bacteria. *Cell* **104**: 143–152.

McKeague AL, Wilson DJ, Nelson J. (2003). Staurosporine-induced apoptosis and hydrogen peroxide-induced necrosis in two human breast cell lines. *Br J Cancer* **88**: 125–131.

Meehl MA, Pinkner JS, Anderson PJ, Hultgren SJ, Caparon MG. (2006). A novel endogenous inhibitor of the secreted streptococcal NAD-glycohydrolase. *PLoS Pathog* **1**: e35.

Michos A, Gryllos I, Hakansson A, Srivastava A, Kokkotou E, Wessels MR. (2006). Enhancement of streptolysin O activity and intrinsic cytotoxic effects of the group A streptococcal toxin, NAD-glycohydrolase. *J Biol Chem* **281**: 8216–8223.

Miettinen M, Lehtonen A, Julkunen I, Matikainen S. (2000). Lactobacilli and Streptococci activate NF-kappa B and STAT signaling pathways in human macrophages. *J Immunol* **164**: 3733–3740.

Molinari G, Rohde M, Talay SR, Chhatwal GS, Beckert S, Podbielski A. (2001). The role played by the group A streptococcal negative regulator Nra on bacterial interactions with epithelial cells. *Mol Microbiol* **40**: 99–114.

Mora M, Bensi G, Capo S, Falugi F, Zingaretti C, Manetti AG *et al.* (2005). Group A *Streptococcus* produce pilus-like structures containing protecive antigens and Lancefield T antigens. *Proc Natl Acad Sci USA* **102**: 15641–15646.

Musser JM, DeLeo FR. (2005). Toward a genome-wide systems biology analysis of host–pathogen interactions in group A *Streptococcus*. *Am J Pathol* **167**: 1461–1472.

Nakagawa I, Nakata M, Kawabata S, Hamada S. (2001). Cytochrome c-mediated caspase-9 activation triggers apoptosis in *Streptococcus pyogenes*-infected epithelial cells. *Cell Microbiol* **3**: 395–405.

Nakagawa I, Nakata M, Kawabata S, Hamada S. (2004). Transcriptome analysis and gene expression profiles of early apoptosis-related genes in *Streptococcus pyogenes*-infected epithelial cells. *Cell Microbiol* **6**: 939–952.

Nakata M, Podbielski A, Kreikemeyer B. (2005). MsmR, a specific positive regulator of the *Streptococcus pyogenes* FCT pathogenicity region and cytolysin-mediated translocation system genes. *Mol Microbiol* **57**: 786–803.

Nizet V. (2002). Streptococcal beta-hemolysins: genetics and role in disease pathogenesis. *Trends Microbiol* **10**: 575–580.

Ozeri V, Rosenshine I, Ben-Ze'Ev A, Bokoch GM, Jou TS, Hanski F. (2001). *De novo* formation of focal complex-like structures in host cells by invading Streptococci. *Mol Microbiol* **41**: 561–573.

Pancholi V, Fischetti VA. (1997). Cell-to-cell signaling between group A streptococci and pharyngeal cells. Role of streptococcal surface dehydrogenase (SDH). *Adv Exp Med Biol* **418**: 499–504.

Podbielski A, Woischnik M, Leonard BA, Schmidt KH. (1999). Characterization of nra, a global negative regulator gene in group A streptococci. *Mol Microbiol* **31**: 1051–1064.

Purushothaman SS, Wang B, Cleary PP. (2003). M1 protein triggers a phosphoinositide cascade for group A *Streptococcus* invasion of epithelial cells. *Infect Immun* **71**: 5823–5830.

Rosini R, Rinaudo CD, Soriani M, Lauer P, Mora M, Maione D *et al.* (2006). Identification of novel genomic islands coding for antigenic pilus-like structures in *Streptococcus agalactiae*. *Mol Microbiol* **61**: 126–141.

Shelburne III SA, Sumby P, Sitkiewicz I, Granville C, DeLeo FR, Musser JM. (2005). Central role of a bacterial two-component gene regulatory system of previously unknown function in pathogen persistence in human saliva. *Proc Natl Acad Sci USA* **102**: 16037–16042.

Sierig G, Cywes C, Wessels MR, Ashbaugh CD. (2003). Cytotoxic effects of streptolysin O and streptolysin S enhance the virulence of poorly encapsulated group a streptococci. *Infect Immun* **71**: 446–455.

Telford JL, Barocchi MA, Margarit I, Rappuoli R, Grandi G. (2006). Pili in Gram-positive pathogens. *Nat Rev Microbiol* **4**: 509–519.

Tsai PJ, Lin YS, Kuo CF, Lei HY, Wu JJ. (1999). Group A *Streptococcus* induces apoptosis in human epithelial cells. *Infect Immun* **67**: 4334–4339.

Virtaneva K, Porcella SF, Graham MR, Ireland RM, Johnson CA, Ricklefs SM *et al.* (2005). Longitudinal analysis of the group A *Streptococcus* transcriptome in experimental pharyngitis in cynomolgus macaques. *Proc Natl Acad Sci USA* **102**: 9014–9019.

Wang B, Li S, Southern PJ, Cleary PP. (2006). Streptococcal modulation of cellular invasion via TGF-beta1 signaling. *Proc Natl Acad Sci USA* **103**: 2380–2385.

Supplementary Information accompanies the paper on The ISME Journal website (http://www.nature.com/ismej)